ELSEVIER

Chemical Geology 175 (2001) 653–671

CHEMICAL GEOLOGY
INCLUDING
ISOTOPE GEOSCIENCE

www.elsevier.com/locate/chemgeo

Precise K–Ar, $^{40}Ar/^{39}Ar$, Rb–Sr and U/Pb mineral ages from the 27.5 Ma Fish Canyon Tuff reference standard

Marvin A. Lanphere [a,*], H. Baadsgaard [b]

[a] *US Geological Survey, 345 Middlefield Road, MS-937, Menlo Park, CA 94025, USA*
[b] *Department of Earth and Atmospheric Sciences, University of Alberta, Edmonton, Canada AB T6G 2E3*

Received 16 September 1999; accepted 1 May 2000

Abstract

The accuracy of ages measured using the $^{40}Ar/^{39}Ar$ technique is affected by uncertainties in the age of radiation fluence-monitor minerals. At present, there is lack of agreement about the ages of certain minerals used as fluence monitors. The accuracy of the age of a standard may be improved if the age can be measured using different decay schemes. This has been done by measuring ages on minerals from the Oligocene Fish Canyon Tuff (FCT) using the K–Ar, $^{40}Ar/^{39}Ar$, Rb–Sr and U/Pb methods. K–Ar and $^{40}Ar/^{39}Ar$ total fusion ages of sanidine, biotite and hornblende yielded a mean age of 27.57 ± 0.36 Ma. The weighted mean $^{40}Ar/^{39}Ar$ plateau age of sanidine and biotite is 27.57 ± 0.18 Ma. A biotite–feldspar Rb–Sr isochron yielded an age of 27.44 ± 0.16 Ma. The U–Pb data for zircon are complex because of the presence of Precambrian zircons and inheritance of radiogenic Pb. Zircons with $^{207}Pb/^{235}U < 0.4$ yielded a discordia line with a lower concordia intercept of 27.52 ± 0.09 Ma. Evaluation of the combined data suggests that the best age for FCT is 27.51 Ma. Published by Elsevier Science B.V.

Keywords: Mineral standards; K–Ar dating; Rb–Sr dating; U–Pb method

1. Introduction

The precision of age measurements by most of the principal decay schemes is now substantially better than accuracy. For example, the analytical precision of $^{40}Ar/^{39}Ar$ ages is commonly better than $\pm 0.25\%$. However, the $^{40}Ar/^{39}Ar$ technique is a relative dating method, in which the age of a mineral is calculated relative to the age of a mineral standard (neutron fluence monitor). Thus, the ultimate accuracy of the method is limited by the accuracy with which the ages of mineral standards used as fluence monitors are known.

Recently, considerable attention has been focused on systematic errors in $^{40}Ar/^{39}Ar$ geochronology (see for example Min et al., 2000). The principal sources of systematic errors are the precision and accuracy of ages of mineral standards used as fluence monitors and uncertainties in the ^{40}K decay constants. The decay constants of ^{40}K are currently being investigated, but at present, there is no agreement to change the decay constants.

* Corresponding author. Tel.: +1-650-329-4659; fax: +1-650-329-4664.
E-mail addresses: alder@mojave.wr.usgs.gov, alder@usgs.gov (M.A. Lanphere).

0009-2541/01/$ - see front matter. Published by Elsevier Science B.V.
PII: S0009-2541(00)00291-6

There is lack of agreement about the ages of certain mineral standards used as fluence monitors. The ages of monitor minerals measured in the USGS Menlo Park laboratory and those reported by Renne et al. (1998) differ by nearly 2%. Lanphere and Dalrymple (2000) made first-principles calibrations of ^{38}Ar tracers using measured quantities of commercial purified air Ar. These tracers were then used to calibrate the $^{40}Ar_{rad}$ content of a primary mineral standard. Two laboratories in Japan that have made first-principles calibrations of ^{38}Ar tracers report good agreement with the $^{40}Ar_{rad}$ content of a primary mineral standard determined in the Menlo Park laboratory (Lanphere and Dalrymple, 2000). In contrast, the $^{40}Ar_{rad}$ content of the primary mineral standard, GA1550 biotite, adopted by Renne et al. (1998) has been calibrated by first principles in only one laboratory. Lanphere and Dalrymple (2000) concluded that it is unwise to use the values suggested by Renne et al. (1998) for ages of fluence monitors until the $^{40}Ar_{rad}$ content of their primary standard is measured by first principles in another laboratory.

An impasse exists in the K–Ar and $^{40}Ar/^{39}Ar$ ages of primary mineral standards, and this impasse carries over to the ages of secondary mineral standards derived by intercalibration or determined independently. The lack of agreement on the ages of minerals used as fluence monitors is a systematic error, affecting the accuracy of $^{40}Ar/^{39}Ar$ ages. It is important to eliminate this systematic error. An alternative way to determine the accuracy of the age of a mineral standard is to measure ages using different parent–daughter decay systems. If two or more radiometric clocks, that is, different radiometric dating methods, running at different rates, give the same age, this is powerful evidence that the age is correct. This was the objective of the current project in which we measured the ages of minerals from the Fish Canyon Tuff (FCT) using the K–Ar, Rb–Sr and U–Pb dating methods. Sanidine from the FCT has been used widely as a fluence monitor mineral in $^{40}Ar/^{39}Ar$ dating. That is why it is particularly important to establish an accurate age for the FCT.

The Oligocene FCT (see Lipman, 1975; Whitney and Stormer, 1985) was erupted from the La Garita caldera, part of the central caldera complex of the San Juan Mountains of southwestern Colorado. The FCT is a vast ash-flow sheet of uniform, phenocryst-rich, dacite that had a volume of about 5000 km^3. Several preparations of minerals from the FCT have been made by us and by other workers. All of the samples used in this work were collected in the same area on the north side of Colorado Highway 160, opposite Fun Valley Resort west of South Fork, Colorado.

2. K–Ar and $^{40}Ar/^{39}Ar$ analyses

K–Ar and $^{40}Ar/^{39}Ar$ ages were measured on sanidine, biotite and hornblende separated from 79COLE-5 collected by P.W. Lipman, on FCT-2 sanidine and biotite and FCT-3 biotite prepared by J. F. Sutter and M. J. Kunk from samples collected at the same location, on FCT87 sanidine and biotite collected and prepared by H. Baadsgaard in 1987, on FCT92 biotite collected and prepared by H. Baadsgaard in 1992, and on FCT (BGC) sanidine prepared by P. R. Renne. All ages are relative to an intralaboratory standard, SB-3 biotite, whose age of 162.9 ± 0.9 Ma was determined using ^{38}Ar tracers calibrated against purified air Ar using first principles (Lanphere and Dalrymple, 2000). The analytical procedures for K–Ar dating were described by Dalrymple and Lanphere (1969) and Hildreth and Lanphere (1994) and the analytical procedures for $^{40}Ar/^{39}Ar$ dating were described by Dalrymple and Duffield (1988) and Lanphere (2000).

The decay constants for ^{40}K are: $\lambda_\varepsilon = 4.962 \times 10^{-10}$ $year^{-1}$ and $\lambda_\beta = 0.581 \times 10^{-10}$ $year^{-1}$ (Beckinsale and Gale, 1969). The isotopic abundance of ^{40}K is 1.167×10^{-4} mol/mol (Garner et al., 1976).

K–Ar ages of biotite and hornblende from 79COLE-5 are 27.55 ± 0.34 and 27.53 ± 0.46 Ma, respectively (Table 1). $^{40}Ar/^{39}Ar$ total fusion ages of bulk samples of sanidine and biotite from 79COLE-5

Table 1
K–Ar ages and analytical data for biotite and hornblende from sample 79COLE-5

Mineral	K_2O (wt.%)	$^{40}Ar_{rad}$ (10^{-10} mol/g)	$^{40}Ar_{rad}$ (%)	Age (Ma)
Biotite	9.235 ± 0.015	3.691	81.9	27.55 ± 0.34
Hornblende	0.857 ± 0.001	0.3423	52.3	27.53 ± 0.46

Table 2
$^{40}Ar/^{39}Ar$ ages and analytical data for bulk samples of sanidine and biotite from sample 79COLE-5

$^{40}Ar/^{39}Ar$	$^{37}Ar/^{39}Ar$	$^{36}Ar/^{39}Ar$	$^{40}Ar_{rad}$ (%)	$^{39}Ar_{Ca}$ (%)	$^{36}Ar_{Ca}$ (%)	K/Ca	Age (Ma)
Sanidine [J = 0.0069475] — 0.3808 g							
2.419	0.008253	0.0006969	91.3	< 0.001	0.31	59.4	27.46 ± 0.34
Biotite [J = 0.0043127] — 0.2613 g							
4.713	0.02300	0.003787	76.2	0.002	0.16	21.3	27.72 ± 0.42

are 27.46 ± 0.34 and 27.72 ± 0.42 Ma, respectively (Table 2). All analytical errors cited in this paper are $\pm 2\sigma$.

Laser-fusion $^{40}Ar/^{39}Ar$ ages were measured on 2–6 grains of several preparations of sanidine and biotite from FCT. The usual practice is to fuse 4–6 aliquants of grains and then pool the ages of the individual aliquants. Six aliquants of sanidine and four aliquants of biotite from 79COLE-5 yielded pooled ages of 27.62 ± 0.13 and 27.62 ± 0.16 Ma, respectively (Table 3).

A comparison of several preparations of minerals from the FCT was made in March 1997 utilizing laser fusion on 4–8 grains. Sanidine from the Taylor Creek Rhyolite of New Mexico (age = 27.92 Ma) was used as the flux-monitor mineral. The Taylor Creek sanidine is a secondary standard that was calibrated using SB-3 biotite as the primary standard. The $^{40}Ar/^{39}Ar$ ages are given in Table 4, and the numbers in parentheses are the number of aliquants of each mineral separate that were fused.

Five $^{40}Ar/^{39}Ar$ incremental-heating experiments were made on sanidine and biotite from three different preparations of FCT. Samples were heated to a series of temperatures in a resistance-heated furnace, and an apparent age was calculated for the gas extracted at each temperature. In calculating an apparent age, it was assumed that the non-radiogenic Ar in a sample is of atmospheric isotopic composition. The data from incremental-heating experiments are commonly displayed on either an age spectrum diagram or on isotope correlation diagrams. The derivative ages for an incremental-heating experiment are the plateau age for the age spectrum diagram, the isochron age on the $^{40}Ar/^{36}Ar$ vs. $^{39}Ar/^{36}Ar$ isotope correlation diagram, and the inverse isochron age on the $^{36}Ar/^{40}Ar$ vs. $^{39}Ar/^{40}Ar$ isotope correlation diagram. Diagrams for 79COLE-5 sanidine are shown in Fig. 1a–c. The analytical data for 79COLE-5 sanidine are given in Table 5.

The various ages for the five incremental-heating experiments are given in Table 6. The plateau and

Table 3
Laser-fusion $^{40}Ar/^{39}Ar$ ages and analytical data for sanidine and biotite from sample 79COLE-5

$^{40}Ar/^{39}Ar$	$^{37}Ar/^{39}Ar$	$^{36}Ar/^{39}Ar$	$^{40}Ar_{rad}$ (%)	$^{39}Ar_{Ca}$ (%)	$^{36}Ar_{Ca}$ (%)	K/Ca	Age (Ma)
Sanidine [J = 0.003545]							
4.398	0.009359	0.0001344	99.1	< 0.001	1.6	52.4	27.65 ± 0.32
4.375	0.01052	0.0000578	99.6	< 0.001	4.2	46.6	27.65 ± 0.32
4.389	0.01157	0.0001816	98.8	< 0.001	1.5	42.4	27.51 ± 0.32
4.388	0.01113	0.0001290	99.1	< 0.001	2.0	44.0	27.60 ± 0.32
4.403	0.01225	0.000161	98.9	< 0.001	1.8	40.0	27.64 ± 0.32
4.388	0.01194	0.000107	99.3	< 0.001	2.6	41.0	27.64 ± 0.32
						Mean age:	27.62 ± 0.13
Biotite [J = 0.00347]							
4.933	0.02365	0.001636	90.2	0.0015	0.34	20.7	27.64 ± 0.34
4.920	0.02318	0.001616	90.3	0.0015	0.33	21.1	27.60 ± 0.32
4.899	0.02178	0.0015	90.9	0.0014	0.34	22.5	27.65 ± 0.32
4.860	0.003547	0.001409	91.4	0.0023	0.59	13.8	27.61 ± 0.32
						Mean age:	27.62 ± 0.16

Table 4
Laser-fusion ages for sanidine and biotite from several different samples of FCT

Mineral	Age (Ma)
FCT (BGC) sanidine	27.70 ± 0.14 (6)
FCT87 sanidine	27.54 ± 0.16 (6)
FCT87 biotite	27.41 ± 0.14 (6)
FCT92 biotite	27.70 ± 0.20 (6)
79COLE-5 sanidine	27.76 ± 0.14 (6)
79COLE-5 biotite	27.67 ± 0.16 (6)

isotope correlation (isochron) ages for the five minerals are in excellent agreement. Isochron ages are preferred because they do not require any assumption about the isotopic composition of non-radiogenic Ar in the mineral. For the five minerals, the intercepts of the isochrons agreed with the value of atmospheric $^{40}Ar/^{36}Ar$ within $\pm 2\sigma$. The weighted mean age (Taylor, 1982) of the plateau and isochron ages is 27.57 ± 0.18 Ma.

3. Rb–Sr dating of biotite and feldspar

A Rb–Sr age was determined for the FCT using biotite and cogenetic feldspar to obtain an isochron

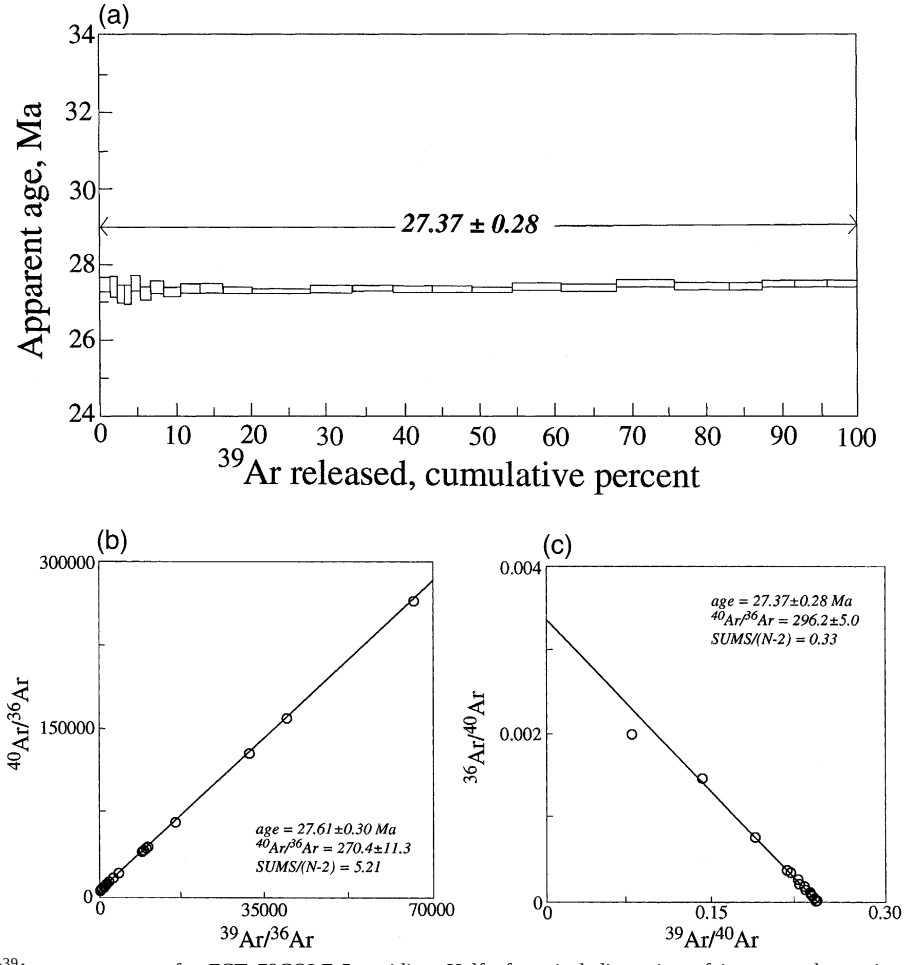

Fig. 1. (a) $^{40}Ar/^{39}Ar$ age spectrum for FCT 79COLE-5 sanidine. Half of vertical dimension of increment boxes is estimated standard deviation of increment age. (b) Isotope correlation diagram (isochron) for FCT 79COLE-5 sanidine. SUMS is the weighted sum of the squares of the residuals (York, 1969). (c) Isotope correlation diagram (inverse isochron) for FCT 79COLE-5 sanidine.

Table 5
Analytical data for incremental-heating experiment on 79COLE-5 Sanidine

[J = 0.00377747]

Temperature (°C)	$^{40}Ar/^{39}Ar$	$^{37}Ar/^{39}Ar$	$^{36}Ar/^{39}Ar$	Moles $^{40}Ar_{rad}$	$^{40}Ar_{rad}$ (%)	$^{39}Ar_{Ca}$ (%)	$^{36}Ar_{Ca}$ (%)	K/Ca	^{39}Ar (%)	Age (Ma)	±s.d.
450	12.690	0.5841	0.02556	1.459E-15	40.8	0.070	0.040	0.61	0.839	34.91	±16.8
500	7.076	0.18648	0.010437	1.357E-14	56.5	0.13	0.013	0.48	2.63	27.03	±1.40
575	4.574	0.006223	0.001713	3.700E-14	88.7	0.19	0.000	0.097	78.7	27.43	±0.54
600	4.492	0.16018	0.001582	4.152E-14	89.7	0.20	0.011	2.7	3.06	27.23	±0.48
625	4.372	0.03539	0.001153	3.841E-14	92.1	0.20	0.002	0.82	13.8	27.20	±0.52
650	4.341	0.02829	0.000893	5.102E-14	93.8	0.20	0.002	0.84	17.3	27.51	±0.40
675	4.282	0.07065	0.000843	5.972E-14	94.1	0.21	0.005	2.2	6.94	27.24	±0.36
700	4.245	0.008886	0.000604	7.546E-14	95.6	0.21	0.001	0.39	55.1	27.42	±0.30
725	4.178	0.06351	0.000462	9.754E-14	96.6	0.21	0.004	3.7	7.72	27.29	±0.26
750	4.153	0.06841	0.000335	1.119E-13	97.5	0.21	0.005	5.4	7.16	27.38	±0.24
775	4.137	0.12887	0.000300	1.397E-13	97.9	0.21	0.009	11.4	3.80	27.37	±0.22
800	4.116	0.05595	0.000230	1.661E-13	98.2	0.22	0.004	6.5	8.76	27.33	±0.20
825	4.174	0.05604	0.000453	3.454E-13	96.7	0.21	0.004	3.3	8.74	27.28	±0.18
840	4.143	0.002845	0.000295	2.342E-13	97.7	0.21	0.000	0.26	172.2	27.35	±0.18
855	4.089	0.03372	0.000108	2.268E-13	99.1	0.22	0.002	8.3	14.5	27.38	±0.18
870	4.083	0.04708	0.000109	2.270E-13	99.1	0.22	0.003	11.5	10.4	27.34	±0.18
885	4.083	0.06430	0.000114	2.367E-13	99.1	0.22	0.004	15.0	7.62	27.34	±0.18
900	4.081	0.04437	0.000117	2.455E-13	99.0	0.22	0.003	10.1	11.0	27.31	±0.18
915	4.092	0.06285	0.000119	2.832E-13	99.0	0.22	0.004	14.0	7.80	27.39	±0.18
930	4.086	0.04297	0.000113	3.044E-13	99.0	0.22	0.003	10.1	11.4	27.35	±0.18
945	4.231	0.04912	0.000554	3.422E-13	96.0	0.21	0.003	2.4	9.98	27.45	±0.18
955	4.086	0.06517	0.000112	3.218E-13	99.1	0.22	0.004	15.5	7.52	27.36	±0.18
965	4.077	0.003643	0.000063	1.873E-13	99.3	0.22	0.000	1.5	134.5	27.37	±0.20
980	4.073	0.003801	0.000016	1.801E-13	99.7	0.22	0.000	6.2	128.9	27.43	±0.20
1000	4.078	0.003523	0.000033	1.943E-13	99.6	0.22	0.000	2.9	139.1	27.43	±0.20
1050	4.074	0.003853	0.000026	1.777E-13	99.6	0.22	0.000	3.9	127.2	27.42	0.20

slope. An essentially two-point isochron is obtained unless the biotite is of variable purity or Rb-content. To test the effect of sample impurities on the Rb–Sr data, the biotite was purified in increasing stages and analyzed at each stage (see Table 7). After magnetic separation, during which, the more abundant hornblende was not removed, a single heavy-liquid separation yielded fairly impure biotite. The gravity separation was repeated with only slight improvement in sample purity. In the next stage, different aliquots of the preceding separate were ground lightly under acetone, washed in water and again subjected to

Table 6
Summary of age spectrum and isotope correlation ages for minerals from the FCT

Mineral	Plateau age (Ma)	Plateau ^{39}Ar[a] (% [steps])	Isochron age (Ma)	Inverse age (Ma)
79COLE-5 sanidine	27.37 ± 0.28	100 [27 of 27]	27.61 ± 0.30	27.37 ± 0.28
79COLE-5 biotite	27.47 ± 0.40	99 [5 of 8]	27.62 ± 0.52	27.64 ± 0.48
FCT-2 sanidine	27.55 ± 0.20	99 [7 of 9]	27.70 ± 0.32	27.58 ± 0.28
FCT-2 biotite	27.55 ± 0.24	98 [6 of 8]	27.97 ± 0.28	27.96 ± 0.28
FCT-3 biotite	27.42 ± 0.34	100 [12 of 13]	27.35 ± 0.38	27.37 ± 0.38

Plus-or-minus values are two standard deviations of analytical precision (2σ).
[a]% is proportion of total ^{39}Ar defining plateau. Steps are number of gas increments on plateau.

heavy liquid separation. This procedure removed most of the remaining hornblende, and the biotite separate improved markedly in purity. The remaining separate was sieved into two size ranges and (A) subjected to vibration and rolling away of rounded grains on a stiff paper and (B) thoroughly ground under acetone and washed. These two latter procedures produced the purest biotite separates. The data for sequential analyses are given in Table 7 and shown in a Sr evolution diagram (Fig. 2). The slope produced by a regression of all the sample data yielded an isochron age of 27.39 ± 0.12 (2σ) Ma, and that obtained using only the best biotite with the feldspars yielded an isochron age of 27.44 ± 0.16 (2σ) Ma with an initial $^{87}Sr/^{86}Sr$ ratio = 0.70635 ± 0.00016 (2σ). The effect of the impurities is to move the data along the isochron. It is difficult to remove all impurities from the biotite because it contains inclusions of apatite and occasional feldspar (see Fig. 3). Any small amount of impurities remaining in the "best" samples should not influence the age significantly.

Analytical notes: The Rb–Sr analyses were carried out using a mixed ^{84}Sr–^{87}Rb spike. The ^{84}Sr-spike was calibrated against NBS SRM 988, and the ^{87}Rb was 99.8% pure ^{87}Rb obtained from Oak Ridge National Laboratory. The mixed spike was check-calibrated for Sr with NBS SRM 987 standard $SrCO_3$, and the ^{87}Rb vs. Johnson–Matthey "Spec–pure" normal rubidium chloride. The spike calibration and analytical procedures (Cavell, 1986) were checked by periodically analyzing NBS SRM 607 K-feldspar with the following results (up to and during the period of the FCT analyses):

	NBS Certificate of Analysis	*Comparison results*
Rubidium	523.90 ± 1.01 (2σ) ppm	523.8 ± 1.4 (2σ) ppm
Strontium	65.485 ± 0.320 (2σ) ppm	65.37 ± 0.16 (2σ) ppm
Isotopic ratio $^{87}Sr/^{86}Sr$	1.20039 ± 0.00020 (2σ)	1.20098 ± 0.00032 (2σ) (normalized to NBS 987 = 0.71024)

Parameters for the regression of Rb–Sr isochrons were derived from 16 analyses of the standard. The standard deviation ($\pm 1\sigma$) of the $^{87}Rb/^{86}Sr$ ratio is ± 2.25‰ and that for the $^{87}Sr/^{86}Sr$ ratio is 0.222‰. The calculated correlation coefficient is 0.56. The decay constant used is $\lambda\ (^{87}Rb) = 1.42 \times 10^{-11}$ year^{-1} (Davis et al., 1977).

4. Uranium–lead dating of FCT zircons

4.1. Macrobomb method on large bulk samples

Zircon (containing abundant inclusions) was separated from a 100-kg sample of the FCT (FCT87) by crushing, sieving and a repeated combination of heavy liquid and magnetic separation. A portion of acid-washed purified bulk zircon was ground in a cleaned agate mortar to an impalpable powder and then stirred in the mortar to homogenize it. The remainder of the unground bulk zircon sample was sieved into various size fractions. To remove occluded HF-soluble impurities, such as feldspar and apatite, aliquots from several size fractions were ground, washed with concentrated HNO_3, with cold, concentrated HF and thoroughly with H_2O before analysis.

Analytical notes: The method used 20 ml of HF–HNO_3 dissolution medium in a 25 ml teflon bomb (Macrobomb), but the procedure of Krogh (1973) was varied by coprecipitating Pb with highly-purified $Ba(NO_3)_2$ (see Cavell, 1986). A mixed ^{208}Pb–^{235}U isotope tracer or spike was added to an aliquot of the dissolved zircon sample to obtain U–Pb concentrations. A solution prepared from enriched ^{235}U (99.74% ^{235}U obtained from Oak Ridge National Laboratory) was calibrated vs. a standard solution prepared from NBS SRM 950a U_3O_8 (normal isotope abundance). A solution prepared from enriched ^{208}Pb (99.75% ^{208}Pb obtained from Oak Ridge National Laboratory) was calibrated vs. standard solutions prepared from NBS SRM standard leads of three kinds: "equal atom lead" (982), radio-

Table 7
FCT Rb–Sr Isotope analyses (in order of purification and analysis)

Sample	^{87}Rb	^{86}Sr	$^{87}Rb/^{86}Sr$	$^{87}Sr/^{86}Sr \pm 2\sigma$
Plagioclase	1.38	101.5	0.0135	0.70641 ± 6
Plagioclase-rpt	1.42	97.08	0.0144	0.70633 ± 4
Sanidine	19.77	90.98	0.215	0.70642 ± 15
Sanidine-rpt	18.49	85.35	0.214	0.70640 ± 6
Initial single separation of biotite				
Biotite 1	79.86	4.049	19.28	0.71395 ± 6
Biotite 2	80.43	4.197	18.95	0.71368 ± 8
Biotite 3	74.47	4.374	16.67	0.71288 ± 4
Biotite 4	73.47	4.465	16.11	0.71278 ± 5
Biotite 5	74.63	4.406	16.58	0.71300 ± 2
Biotite 6	62.82	5.133	11.99	0.71123 ± 6
Repurification of first batch				
Biotite A	84.39	3.064	27.23	0.71701 ± 10
Biotite B	85.44	3.159	26.74	0.71698 ± 6
Biotite C	81.29	3.510	22.89	0.71547 ± 10
Biotite D	78.00	3.644	21.16	0.71439 ± 12
Biotite E	76.96	3.804	20.00	0.71416 ± 26
Biotite F	77.16	3.754	20.32	0.71445 ± 8
Ground lightly under acetone and again separated				
Biotite A +	96.12	1.684	56.41	0.72834 ± 2
Biotite B +	95.55	1.792	52.72	0.72696 ± 12
Biotite A	106.3	1.726	60.90	0.73014 ± 11
Biotite B	107.4	1.746	60.78	0.72996 ± 6
Biotite C	106.7	1.829	57.69	0.72872 ± 14
Biotite D	107.2	1.822	58.17	0.72909 ± 20
Biotite E	106.63	1.880	56.06	0.72807 ± 6
B 60–80 NR	105.02	1.719	60.41	0.73003 ± 6
B140–80 NR	103.70	1.725	59.42	0.72962 ± 4
Two purifications then rolled (R) (or not (NR)) from stiff paper				
B 60–80 1 R	104.06	1.233	83.42	0.73893 ± 7
B 60–80 2 R	104.36	1.228	84.03	0.73913 ± 5
B 140–80 1 R	101.70	1.274	78.88	0.73698 ± 4
B 140–80 2 R	103.40	1.286	79.47	0.73735 ± 5
Thoroughly ground under acetone and washed				
B > 60 A	106.24	1.286	81.65	0.73815 ± 4
B > 60 B	105.08	1.274	81.54	0.73820 ± 11
B > 60 D	105.46	1.278	82.34	0.73847 ± 5
B 60–100 A	105.88	1.267	82.58	0.73841 ± 9
B 60–100 B	104.69	1.255	82.43	0.73840 ± 5

genic lead (983) and common lead (981). These standard leads were all furnished as pure lead metal for the weighing form, and standard solutions made by simple dissolution in HNO_3. Mass measurements were made on a VG Micromass-30 mass spectrometer, and all lead isotope measurements were normalized to NBS SRM 981 standard lead by mass discrimination corrections, which averaged 0.15% per atomic mass unit. Decay constants used in age computations are: $\lambda^{238}U = 1.55125 \times 10^{-10}$ year^{-1}, $\lambda^{235}U = 9.8485 \times 10^{-10}$ year^{-1} and the atomic ratio $^{238}U/^{235}U = 137.88$ (Jaffey et al., 1971; Shields, 1960).

The results of the analyses are given in Table 8. The repeat analyses of the homogeneous powdered bulk zircon sample show the reproducibility of the measurements and give a measure of the precision of the data.

The data yield a discordia line (see Fig. 4) with concordia intercepts at 27.65 ± 0.34 and 1561 ± 106 Ma (errors $\pm 2\sigma$). The discordance of the data appears to increase with the size of the zircons in the sample. The HF-washed ground samples give results that differ little from those for the unwashed samples, and the loss of acid-soluble lead-bearing inclusions (mainly apatite) does not cause significant variations in data, except for a slight decrease in uranium, radiogenic lead and common lead content. In the bulk samples, there is an "older" lead contaminant, which comes from xenocrystic zircon grains and/or older "cores" or inclusions in the younger zircons. The analyses yielded data that was too discordant for precise age determination, and further work was initiated.

4.2. Microbomb method using ^{205}Pb as isotope dilutant

In 1992, a second sample of FCT was collected close to the first location. Zircon from this second sample was separated and sieved into several size fractions. Portions of the 74–98 and 98–148 μm size fractions were subjected to abrasion (Krogh, 1982) in the presence of pyrite, cleaned and the abraded fractions were analyzed. The best-quality zircons from these abraded fractions were hand-picked for separate analysis; zircons from unabraded coarser-size fractions were also hand-picked for analysis. During picking, there appeared to be three recognizable types of zircons in the FCT: (1) abundant, euhedral, amber-colored with plentiful inclusions and often broken, (2) much less abundant,

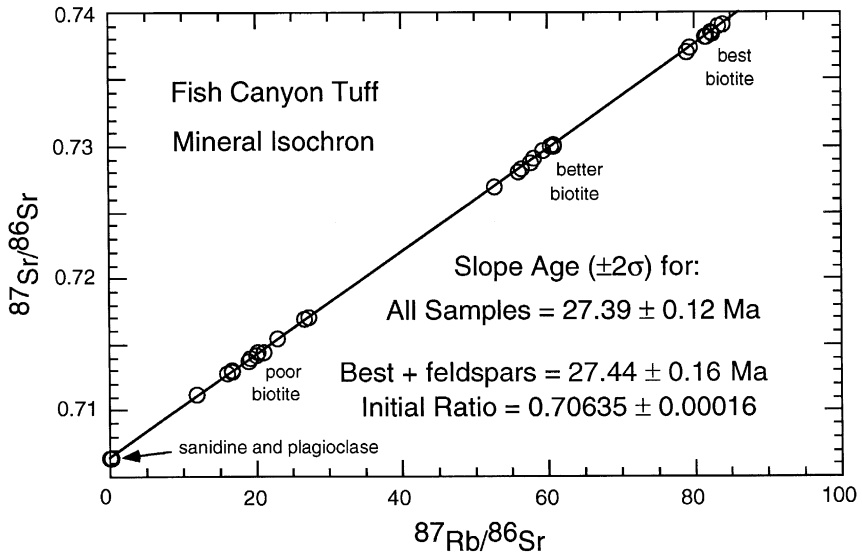

Fig. 2. Sr evolution diagram for analyses of FCT sanidine, plagioclase and biotite of varying purity.

euhedral, pale to colorless with fewer inclusions, and (3) rare, very well-rounded, light to dark-pink grains. Two samples of only amber zircons, one sample containing only "pale" zircons and one sample of the pink well-rounded zircons were picked for analysis.

Analytical notes: The method for U/Pb microbomb (2 ml maximum capacity) analysis was essentially that used by the GSC in Ottawa (Parrish et al., 1987), except that separation of the lead and uranium is accomplished by adsorption on a bead or beads of ion exchange resin introduced directly into

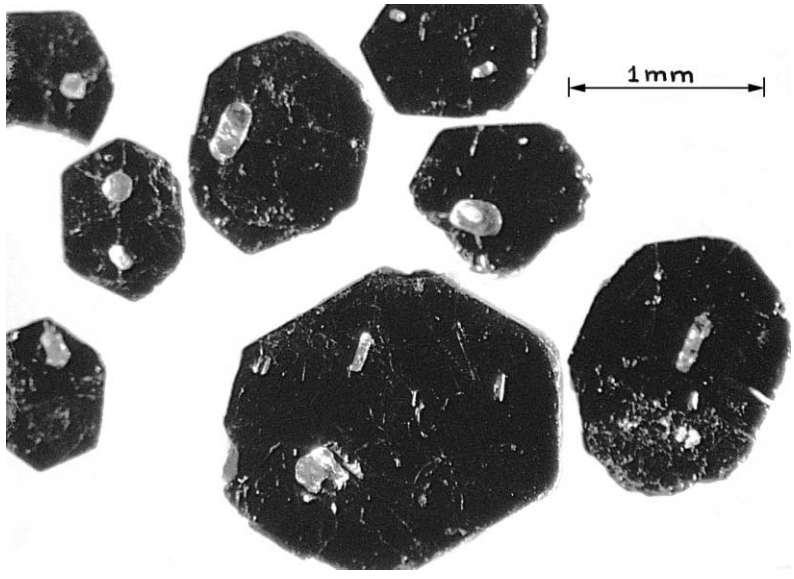

Fig. 3. Inclusions of apatite and feldspar in selected grains of FCT biotite × 36.

Table 8
FCT 87 "bulk" zircon analysis results. "Macrobomb" method with analysis on VG MM-30 mass spectrometer

Sample microns	Weight (mg)	^{206}Pb (ppm)	U (ppm)	Pb-com (ppm)	^{206}Pb/^{238}U	^{207}Pb/^{235}U
Purified bulk sample — all sizes — ground to impalpable powder — homogenized[a]						
Sample-1	53.51	2.222	535.7	0.0535	0.00483	0.0346
Sample-2	64.52	2.229	532.4	0.0814	0.00487	0.0351
Sample-3	158.97	2.224	532.6	0.0214	0.00486	0.0351
Sample-4	69.63	2.215	533.8	0.0184	0.00483	0.0347
Sample-5	68.93	2.219	536.8	0.0168	0.00481	0.0345
Size fractions						
−44	61.18	2.394	598.2	0.0517	0.00466	0.0326
−44	57.16	2.406	600.6	0.0555	0.00466	0.0327
−44	60.14	2.408	601.8	0.0502	0.00466	0.0326
+44–53	56.21	2.270	554.6	0.117	0.00476	0.0340
+44–53	60.74	2.270	553.9	0.0960	0.00477	0.0340
+53–63	54.05	2.137	521.8	0.130	0.00477	0.0340
+53–63	54.76	2.155	530.2	0.171	0.00473	0.0334
+63–74	57.03	2.047	486.1	0.125	0.00490	0.0355
+63–74	46.88	2.019	486.3	0.136	0.00483	0.0348
Size fractions — HF-washed after grinding						
−44	45.27	2.382	595.7	0.0117	0.00465	0.0324
+44–53	56.24	2.211	543.6	0.0235	0.00473	0.0335
+53–63	25.67	2.070	510.4	0.1418	0.00469	0.0329
+74	15.27	1.858	435.2	0.213	0.00497	0.0367

FCT sanidine Pb (normalized) 1:18.440:15.580:37.736.
FCT plagioclase Pb (normalized) 1:18.430:15.576:37.716.
Average Pb used for common Pb 1:18.435:15.578:37.726.
All Pb isotope values normalized to NBS SRM 981.
Pb total blank = 0.80–0.90 ng.
Measurement errors in $207/206 = \pm 0.02\%$ and in $208/206 \pm 0.01\%$.
Common Pb varied from 1.1 to 5.2 ng, ^{206}Pb-rad from 140 to 190 ng and ^{207}Pb-rad from 7.4 to 8.9 ng.
[a]Mean values are ^{206}Pb/^{238}U = 0.00484 ± 6 and ^{207}Pb/^{235}U = 0.0348 ± 6. Reproducibility of ^{206}Pb/^{238}U: $2\sigma = \pm 1.2\%$; and for ^{207}Pb/^{235}U: $2\sigma = \pm 1.7\%$.

the prepared sample solutions (Manton, 1988). A modified method is described by Duke (1993). An aliquot of ^{205}Pb was obtained from T. Krogh (Krogh and Davis, 1975 ; Parrish and Krogh, 1987) and calibrated with the same NBS standards mentioned above for the macrobomb method. Previously calibrated ^{235}U spike solution was added to a suitable amount of ^{205}Pb to make up a mixed ^{205}Pb–^{235}U spike. Mass measurements were made on a VG-354 mass spectrometer and Pb normalized to NBS SRM 981 lead.

The results of the microbomb analyses are given in Table 9. Two concordia diagrams of the data are shown in Fig. 5a and b. The most discordant data points are not included in Fig. 5b.

Results for the analyses of the bulk samples are similar to those from the earlier study. Several of the hand-picked samples yielded more concordant points than the bulk samples, and the pink well-rounded zircons were Precambrian in age. The "pale" zircon sample, picked to give the clearest and "best" zircons, proved to be very highly contaminated with older radiogenic lead (see Fig. 5a). The "pale" sample contained no pink zircons, and the higher content of older radiogenic lead is derived from sources not recognizable under the optical microscope as older exotic material.

4.3. Contamination of the Oligocene FCT zircons with inherited lead

In order for the extrapolated lower discordia–concordia intercept to be interpreted as the age of crys-

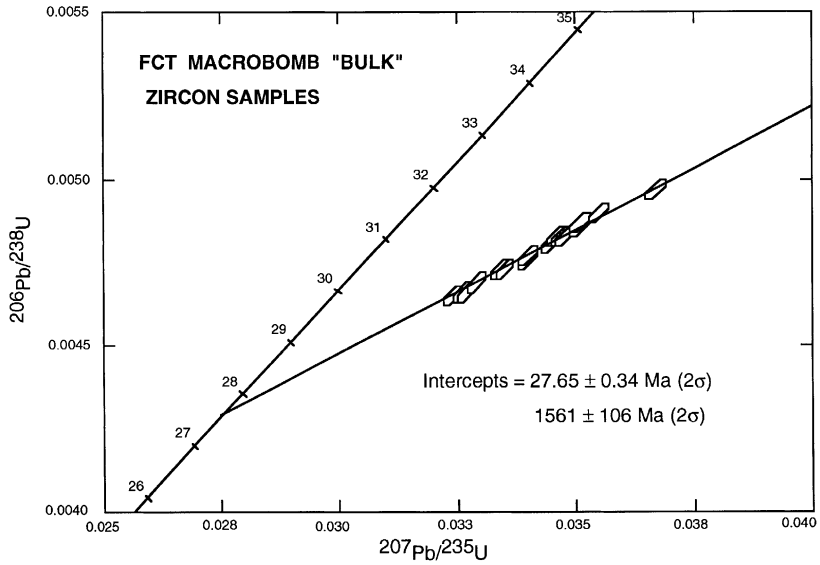

Fig. 4. Concordia plot of U/Pb macrobomb results on FCT87 "bulk" zircon samples.

Table 9
FCT 1992 zircon analyses. A mixed $^{205}Pb + ^{235}U$ isotope dilutant used. "Microbomb" method with isotope analyses on MM-354. AB = abraded, p = picked, amb = amber-colored and lg = large

Sample microns	Weight (mg)	^{206}Pb[a] (ppm)	U (ppm)	Pb-com[b] (ppm)	$^{206}Pb/^{238}U$ ($\pm 1\sigma$% — rms)	$^{207}Pb/^{235}U$ ($\pm 1\sigma$% — rms)
"Bulk" samples						
< 40	5.55	2.252	553	0.0590	0.00474 ± 0.66	0.03356 ± 1.2
< 40	14.26	2.256	559.5	0.0201	0.00469 ± 0.10	0.03311 ± 0.12
40–74	14.32	2.003	468.9	0.0320	0.00497 ± 0.10	0.03654 ± 0.15
40–74	2.76	1.944	460	0.0416	0.00492 ± .03	0.03610 ± 0.17
74–98 AB	7.06	1.704	437.9	0.0981	0.00453 ± 0.48	0.03081 ± 0.71
98–148 AB	3.85	1.768	403.6	0.1645	0.00510 ± 0.21	0.03822 ± 0.44
120–148	5.77	1.381	352.5	0.1963	0.00456 ± 0.53	0.03112 ± 1.0
1987 "Bulk homogeneous sample" (comparison analysis with microbomb)						
Ground < 10 μ	13.47	2.228	534.2	0.0394	0.00485 ± 0.69	0.03510 ± 0.83
Mean values from Table 1	–	2.222	534	0.0383	0.00484 ± 0.6	0.0348 ± 0.6
> 148, p lg amb	0.727	1.023	267.8	0.5624	0.00444 ± 0.19	0.02950 ± 1.3
98–148 AB, p	1.91	1.755	313.4	0.188	0.00652 ± 0.16	0.05710 ± 0.52
98–148, p lg	1.200	1.212	314	0.121	0.00449 ± 0.13	0.03009 ± 0.36
98–148, p amb	0.900	1.203	323	0.038	0.00433 ± 0.11	0.02809 ± 0.65
74–98 AB, p	1.001	1.466	341	0.034	0.00500 ± 0.27	0.03692 ± 0.38
74–98, p	4.70	1.368	342	0.0993	0.00465 ± 0.48	0.03222 ± 0.6
"pale" p	0.850	3.167	229	1.326	0.01607 ± 0.50	0.1797 ± 0.78
"pink" p	0.025	90.32	346	1.404	0.30420 ± 0.05	5.827 ± 0.08

Pb total blank varied from 5.2–11.3 pg.
Corrections for common Pb and mass discrimination same as in Table 1 footnote.
[a]Radiogenic lead after blank and common Pb correction.
[b]Common Pb (feldspar Pb composition used).

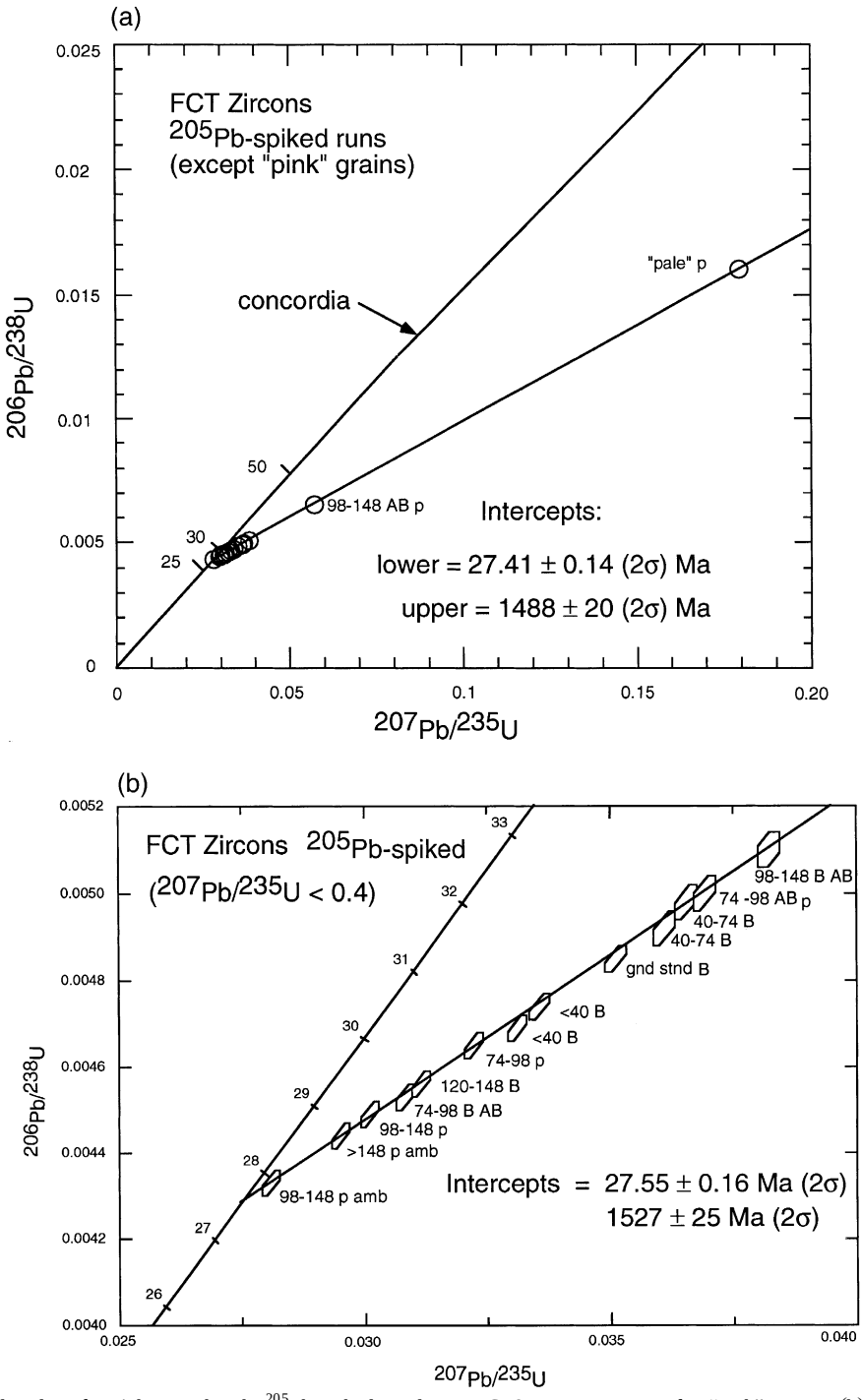

Fig. 5. (a) Concordia plot of U/Pb microbomb–^{205}Pb-spiked results on FCT92 zircons except for "pink" grains. (b) Concordia plot of U/Pb microbomb–^{205}Pb-spiked results on FCT zircons with $^{207}Pb/^{235}U < 0.4$.

tallization of the zircons, the nature, extent and source of the contamination by older radiogenic lead and/or common lead must be ascertained.

4.3.1. Sensitive High Resolution Ion MicroProbe (SHRIMP) analyses of the well-rounded "pink" zircons

Microbomb U/Pb chemical analysis showed the pink zircon sample to be Precambrian in age (see Table 9). A further eight pink zircons were obtained from previously unpicked size fractions of the FCT and individually analyzed for U/Pb on the SHRIMP — model II. A description and the mode of operation of the instrument may be found in Compston et al. (1984), Williams and Claesson (1987), and Stern (1997). An ~25-μm diameter shallow hole was etched on a portion of each polished zircon grain by a focused 25 KV O_2^- beam during mass analysis of the ionized material. Ceylon gem zircon SL13 was used as the standard (Compston and Williams, 1992; Roddick and van Breemen, 1994). The SHRIMP results are given in Table 10 and plotted on a concordia diagram in Fig. 6.

The pink well-rounded zircons are very variable in age, and it is possible that the "pink" zircons are from a source that was variably reset in a later metamorphism around 1400 Ma. They were then incorporated into the FCT when it formed and altered to their present shape. Unless they are removed from the samples, the variability in age of pink contaminant zircon grains makes the establishment of a reliable discordia line very difficult. Fortunately, these colored grains are very easy to recognize and they can be picked from a larger FCT zircon population using a binocular microscope.

4.3.2. SHRIMP analyses on "pale" zircons

To document sources of older radiogenic lead other than the "pink" zircon xenocrysts, a number of non-amber or "pale" zircons were again picked; and 62 zircons from this subset (called FCTL) were mounted, polished for SHRIMP analysis and subjected to cathodoluminescence scanning. From the 62 zircons, some 23 zircons were analyzed with Nos. 2, 7 and 14 analyzed at two sites and No. 13 at three sites. In some cases, the SHRIMP analysis site was

Table 10
FCT U/Pb SHRIMP analyses of selected Precambrian "pink" and "pale" zircons. Correction for common lead made using the 204-method. All errors are $\pm 1\sigma$

Sample	U (ppm)	Th (ppm)	Pb^r (ppm)	206/204 measurement	^{204}Pb (ppb)	$^{206}Pb/^{238}U$	$^{207}Pb/^{235}U$	$^{207}Pb/^{206}Pb$ age (Ma)
"Pink" well-rounded zircons								
FCTH-1.1	212	229	80	4009	14	0.3105 ± 0.0048	4.627 ± 0.093	1767 ± 20
FCTH-2.1	489	31	210	5726	30	0.4153 ± 0.0054	8.154 ± 0.119	2257 ± 9
FCTH-2.2	190	11	78	4387	16	0.4168 ± 0.0086	8.641 ± 0.198	2350 ± 13
FCTH-3.1	206	65	69	5155	11	0.3224 ± 0.0048	4.965 ± 0.089	1827 ± 15
FCTH-4.1	101	54	42	5422	6	0.3716 ± 0.0096	6.672 ± 0.226	2101 ± 34
FCTH-5.1	103	44	45	2535	14	0.3996 ± 0.0075	8.239 ± 0.188	2341 ± 19
FCTH-6.1	260	91	83	5145	13	0.3069 ± 0.0044	4.668 ± 0.081	1805 ± 15
FCTH-7.1	820	4	253	15,092	15	0.3224 ± 0.0039	5.017 ± 0.071	1846 ± 11
FCTH-8.1	424	152	136	10,907	10	0.3073 ± 0.0042	4.600 ± 0.076	1775 ± 14
FCTL-3.1	50	24	18	2242	6	0.3344 ± 0.0083	5.437 ± 0.183	1916 ± 36
Euhedral zircons in "pale" sample								
FCTL-7.1	238	107	56	6926	7	0.2228 ± 0.0041	2.839 ± 0.067	1476 ± 25
FCTL-7.2	278	225	78	6572	9	0.2431 ± 0.0037	3.064 ± 0.058	1455 ± 18
FCTL-13.1	2316	65	517	55,191	8	0.2361 ± 0.0042	2.967 ± 0.072	1450 ± 27
FCTL-13.2	1838	111	392	36,139	10	0.2255 ± 0.0030	2.822 ± 0.050	1442 ± 19
FCTL-13.3	1472	121	282	30,921	8	0.2021 ± 0.0027	2.530 ± 0.045	1442 ± 19
FCTl-18.1	1185	124	361	100,000	3	0.3117 ± 0.0035	4.541 ± 0.059	1725 ± 13

Pb^r is radiogenic Pb.

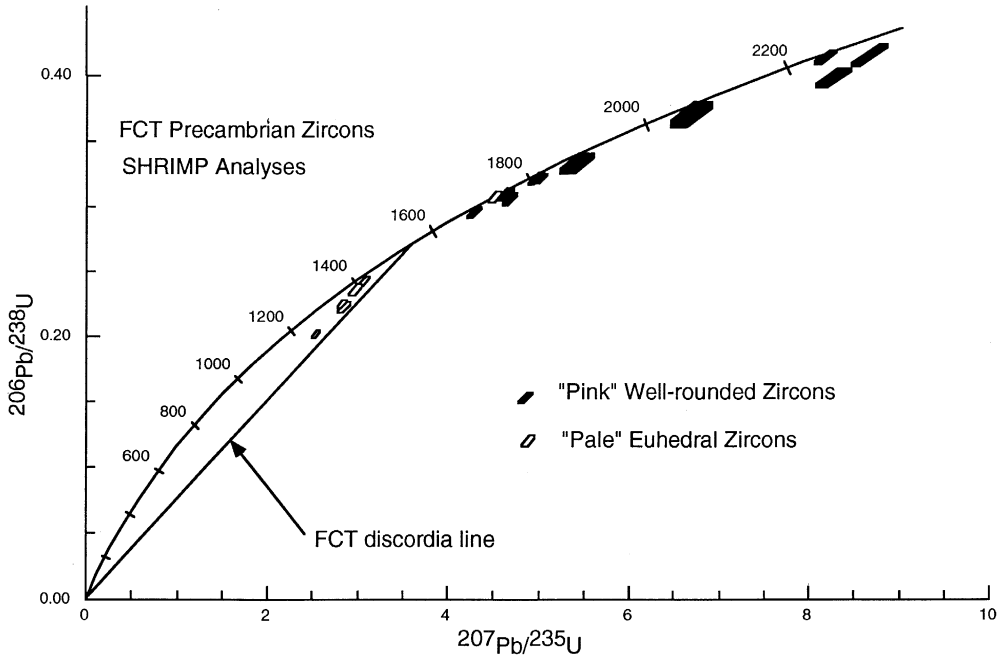

Fig. 6. Concordia plot of SHRIMP analyses yielding Precambrian ages from "pink" and "pale" samples.

chosen to impinge on an inclusion revealed by cathodoluminescence scanning on an electron microscope (see Fig. 7). The results are given in Table 11 (the "pale" FCTL Precambrian zircons are also listed

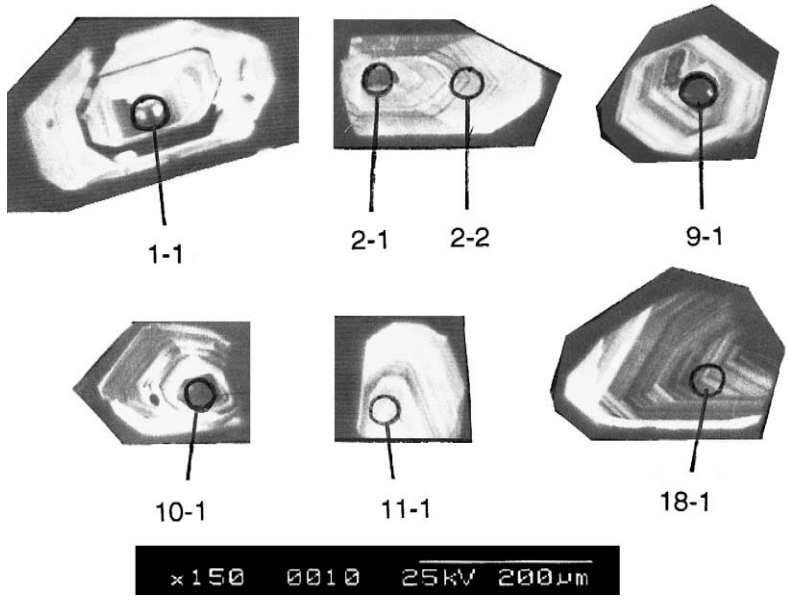

Fig. 7. Cathodoluminescence scans on selected "pale" FCT zircons subjected to SHRIMP analysis. The ring outlines the area of the ionization site. Spot 9-1 is an inclusion with mostly common lead, 18-1 is a Precambrian zircon, 2-2 is an overgrowth ring, while 2-1 is an inherited core on zircon grain 2, 11-1 and 1-1 are small areas containing above-average common lead, and 10-1 appears to be a concordant Cretaceous zircon core.

Table 11
SHRIMP analytical results on FCT "pale" (FCTL) zircons

Site	U (ppm)	Th (ppm)	Pb^r (ppm)	206/204 measurement	^{204}Pb (ppb)	$^{206}Pb/^{238}U \pm 1\sigma$ (204-corrected)	$^{207}Pb/^{235}U \pm 1\sigma$ (204-corrected)	$^{207}Pb/^{206}Pb \pm 1\sigma$ (uncorrected)	$^{238}U/^{206}Pb \pm 1\sigma$ (uncorrected)
1.1	358	241	115	12		0.00391 ± 0.00018	0.00934 ± 0.0112	0.1512 ± 0.0066	214 ± 8
2.1	2387	431	21	1352	14	0.00896 ± 0.00017	0.09406 ± 0.0066	0.0867 ± 0.0024	110 ± 2
2.2	701	374	3	680	4	0.00441 ± 0.00013	0.02413 ± 0.0129	0.0521 ± 0.0019	221 ± 4
3.1	50	24	18	2242	6	0.33444 ± 0.00826	5.43369 ± 0.1825	00.1234 ± 0.0020	2.97 ± 0.07
4.1	554	277	2	342	6	0.00426 ± 0.00011	0.02636 ± 0.0055	0.0882 ± 0.0043	222 ± 5
5.1	834	1295	5	781	4	0.00463 ± 0.00009	0.03339 ± 0.0034	0.0711 ± 0.0029	211 ± 4
6.1	667	310	3	333	8	0.00433 ± 0.00012	0.03599 ± 0.0089	0.0854 ± 0.0036	207 ± 5
7.1	238	107	56	6926	7	0.22281 ± 0.00405	2.83885 ± 0.0673	0.0944 ± 0.0012	4.48 ± 0.08
7.2	278	225	78	6572	9	0.24305 ± 0.0037	3.06374 ± 0.0584	0.09355 ± 0.0008	4.10 ± 0.06
9.1	932	695	3	19	2524	0.00674 ± 0.0013[a]	0.20961 ± 0.0656[a]	0.7725 ± 0.0114	15.1 ± 0.4
10.1	1535	1719	21	2615	3	0.0111 ± 0.0001[a]	0.07515 ± 0.0045[a]	0.0522 ± 0.0012	89.6 ± 1.1
11.1	178	110	1	58	8	0.00431 ± 0.00019	0.04606 ± 0.0139	0.2183 ± 0.0133	189 ± 7
12.1	952	1048	6	1081	4	0.00464 ± 0.00011	0.05738 ± 0.0081	0.0972 ± 0.0068	210 ± 4
13.1	2316	65	517	55,191	8	0.23605 ± 0.0422	2.96740 ± 0720	0.09143 ± 0.0013	4.24 ± 0.08
13.2	1838	111	392	36,139	10	0.22549 ± 0.00299	2.82225 ± 0.0495	0.09116 ± 0.0009	4.43 ± 0.06
13.3	1472	121	282	30,921	8	0.20214 ± 0.00274	2.52985 ± 0.0449	0.09122 ± 0.0009	4.94 ± 0.06
14.1	419	328	2	201	9	0.00443 ± 0.00017	0.01637 ± 0.0094	0.1023 ± 0.0076	204 ± 7
14.2	324	222	2	299	4	0.00450 ± 0.00010	0.02887 ± 0.0038	0.0694 ± 0.0034	216 ± 5
15.1	196	58	1	180	4	0.00424 ± 0.00044	0.02013 ± 0.0468	0.1176 ± 0.0070	212 ± 5
16.1	512	253	3	2275	1	0.00462 ± 0.00009	0.03504 ± 0.0062	0.0614 ± 0.0023	215 ± 4
17.1	454	216	2	631	3	0.00433 ± 0.00010	0.02812 ± 0.0094	0.0704 ± 0.022	225 ± 4
18.1	1185	124	361	10^5	3	0.31172 ± 0.0035	4.54123 ± 0.0587	0.1058 ± 0.0006	3.21 ± 0.04
19.1	511	247	2	864	2	0.00455 ± 0.00015	0.03138 ± 0.0147	0.0654 ± 0.0021	217 ± 4
20.1	610	297	3	4529	1	0.00465 ± 0.00008	0.03829 ± 0.0035	0.0629 ± 0.0018	214 ± 4
21.1	464	197	2	786	2	0.00433 ± 0.00017	0.03797 ± 0.0180	0.0744 ± 0.0053	222 ± 6
22.1	441	214	2	1153	2	0.00450 ± 0.00016	0.03333 ± 0.0164	0.0664 ± 0.0029	219 ± 4
23.1	303	123	1	213	5	0.00414 ± 0.00012	0.01977 ± 0.0058	0.0818 ± 0.0040	226 ± 5

Pb^r is radiogenic lead.
[a] 208-corrected.

in Table 10), and the data obtained for the Precambrian whole zircons plotted in Fig. 6, together with that for the "pink" zircons. These "pale" Precambrian zircons were not recognized as older whole zircons until the SHRIMP analyses, and apparently, result from an igneous event at about 1450 Ma.

To evaluate the type of contaminant lead, earlier TIMS and SHRIMP results on selected "pale" FCT zircons are plotted on a Tera–Wasserburg plot (Tera and Wasserburg, 1972) in Fig. 8a and b. In the full-scale T–W plot (Fig. 8a), the Precambrian zircon grains 3, 7, 13 and 18 may be recognized. Reference lines are drawn from the 27.5 Ma concordia point to that for the FCT feldspar Pb data, and also, for the 18-1 Precambrian contaminant grain data. The inclusion in site 9.1, while containing substantial uranium, has a large amount of common lead, which dominates the isotopic composition of the lead. The inclusion in site 2.1 contains Precambrian contaminant radiogenic lead, whereas the inclusion in site 10.1 appears to be a concordant Late Cretaceous zircon. Sites 1.1 and 11.1 are contaminated by common lead. The TIMS sample called the "pale" zircons is very discordant and contains a substantial older radiogenic lead component. This is not surprising in view of the fact that four euhedral Precambrian zircons were found in only 23 zircons examined by SHRIMP analysis in the second selection of "pale" zircons. In the expanded T–W plot in Fig. 8b are SHRIMP sample sites that do not encompass any noticeable inclusions (as seen on photographs obtained by cathodoluminescence or on the optical microscope). The SHRIMP sample data, ranging between the feldspar lead and radiogenic

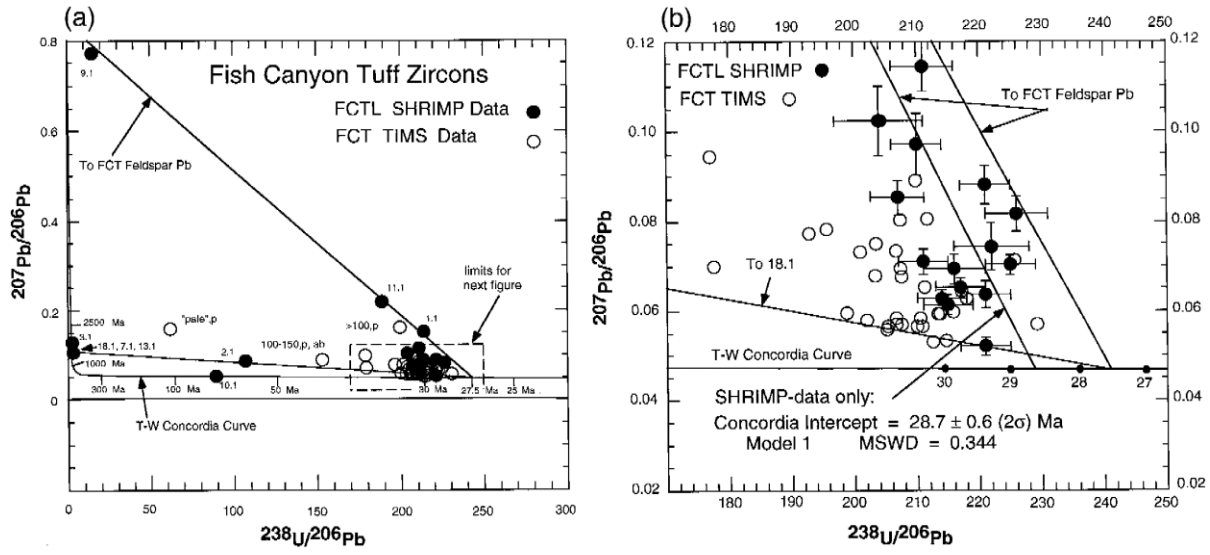

Fig. 8. (a) Tera–Wasserburg plot of FCT zircons analyzed by SHRIMP and TIMS-chemical procedures. The data are the measured results, uncorrected except for the blanks. The error bars all fall within the limit of the sample circles. (b) Tera–Wasserburg plot. Expanded section from Fig. 8a. The 2σ error limits for the SHRIMP analyses are given, while the error limits for the TIMS data points falls on or within the data circle.

lead limits, seem more to be distributed toward the common lead contamination limit, while the TIMS samples show more contamination by old radiogenic lead. This is a result of the sampling and mode of analysis, wherein the TIMS samples are all multi-grain samples, while the SHRIMP samples are thin 25-μm diameter discs taken from an internal portion of single zircons in the clearest part of the polished grain. If the more concordant SHRIMP FCTL data (those shown in Fig. 8b) are subjected to regression (Ludwig, 1991) through the common Pb point for FCT feldspar, a model 1 lower concordia intersection is obtained at 28.7 ± 0.6 Ma (2σ) for the $^{206}Pb/^{238}U$ age. This age does not overlap with the 27.55 ± 0.16 Ma (2σ) normal concordia (lower-intersection) age given in Fig. 5b.

5. Discussion

The least contaminated zircon samples are ostensibly those for the most concordant SHRIMP analyses. However, much attention has been and is being focused on studies of the internal microstructure of zircon in an effort to resolve some of the difficulties encountered even in the precise dating of single zircons (McLaren et al., 1993). A single zircon may consist of several growth phases, whose ages may be related to distinct petrologic events (Sergeev et al., 1995). In the FCT zircons, the inclusions tend to be grouped in definite growth planes. Zoning in zircons gives rise to wide variations in the incorporation of contaminant elements in zircon (Köppel and Grünenfelder, 1971; Sommerauer, 1974; Clark et al., 1979; Pidgeon, 1992; Nasdala et al., 1995). Variation in contaminant P_2O_5 is particularly important, because it can lead to large differences in the uptake of common Pb (Watson et al., 1997). Inherited cores in zircons may also show differences in style of zoning, composition and age compared to their host zircon, and this often reveals they have not undergone significant chemical interaction with either their host zircon or host magmatic melt (Paterson et al., 1992). The problems of secondary loss of radiogenic lead and/or inheritance of older xenocrystic zircon may be avoided if it is possible to analyze only pristine igneous zircon unaffected by Pb loss or inheritance of older zircon (Williams, 1992). For Mesozoic–Cenozoic samples (McClelland and Mattinson, 1996), this is difficult to do precisely by SHRIMP or other microanalytical techniques, such as air abrasion

(Krogh, 1982) and analysis of individual zircon fragments (Steiger et al., 1993). Mattinson (1994) devised a step-wise zircon dissolution procedure, which preferentially removes outer zircon layers susceptible to lead loss, as well as core regions containing inherited zircon and leaves a residue large enough for precise U–Pb analysis.

The discordance shown by most of the FCT zircon samples can be ascribed to contamination by exotic grains of Precambrian zircons, but the SHRIMP analyses (corrected for common lead via the ^{204}Pb isotope) still show discordance for many zircon areas, which do not have evident inclusions. It is possible that older occluded zircon grains are present down to very small grain sizes. Photomicrographs from a typical population of FCT zircons are shown in Figs. 9 and 10. The abundance of inclusions is evident, as well as the fact that many of the inclusions are very small. At high magnification (Fig. 10), it may be seen that some of the inclusions have smaller inclusions of their own. Most of these inclusions are not old zircon. However, simple computation shows that the proportion of older contaminant Precambrian zircon (such as that in sample 18.1) in a younger FCT zircon needs only to be one part in 1500–2500 to account for the apparent contaminant radiogenic lead in many of the SHRIMP samples. A single such contaminant zircon particle is not visible even at the magnification shown in Fig. 10, and there could be a number of yet smaller contaminant zircon particles, which interfere even in SHRIMP analyses.

The FCT zircon discordia line for the microbomb ^{205}Pb-spiked samples runs to the right of the $\sim$1450 Ma grouping of euhedral "pale" zircons (see Fig. 6). A "mean contaminant lead" point probably exists between 1450 and 1725 Ma, the range of the euhedral contaminant zircons. Using 1450 and 1725 Ma as upper limits on a discordia line through each of these points and the average data for the ^{205}Pb-spiked microbomb analyses, one obtains lower intercepts of 27.36 and 28.05 Ma, respectively. The upper intercept of 1527 Ma on the FCT discordia line in Fig. 5b represents an average contamination with old radiogenic lead. In view of the variability of the documented Precambrian isotope lead contamination, the best zircon U/Pb age to be derived from the TIMS data is from a discordia line, which omits the very discordant samples. All the TIMS zircon data with $^{207}\mathrm{Pb}/^{235}\mathrm{U} < 0.4$ yield a discordia line with a lower concordia intercept of 27.52 ± 0.09 Ma (2σ). This lower concordia intercept age depends mostly on the

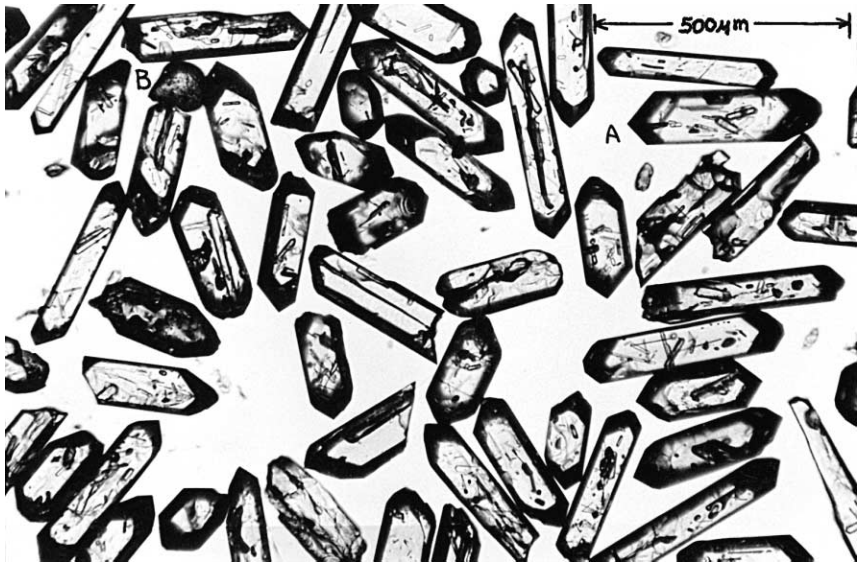

Fig. 9. A typical population of FCT zircons at 90× magnification. Zircon B is a well-rounded "pink" Precambrian zircon. Zircon A is further magnified in Fig. 10.

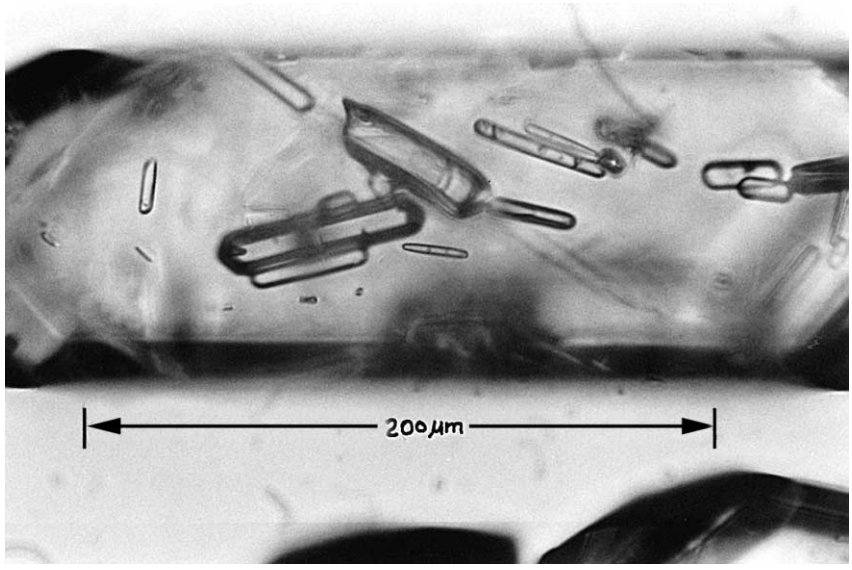

Fig. 10. FCT zircon A from Fig. 9 at about 560 × magnification.

less-contaminated samples, but it is susceptible to errors in tracer calibration, since no standard zircon samples were available for comparison analyses. This age is the best that can be done with the usual discordia treatment of the U/Pb data of this study, but is relatively unsatisfactory for a standard zircon sample, which, ideally should be demonstrably homogeneous and concordant. The Tera–Wasserburg discordia–concordia intercept shown in Fig. 8b (28.7 ± 0.6 Ma) for the SHRIMP analyses of the more concordant FCTL samples could perhaps be the most acceptable result, since it is measured against a carefully checked standard zircon (SL13) and on apparently inclusion-free areas of zircon. This result also compares favorably with a $^{206}Pb/^{238}U$-value of 28.41 ± 0.05 Ma (2σ) by Oberli et al. (1990) for carefully selected single zircons from the FCT. However, The SHRIMP result is obtained on a selected population of zircons that could be petrologically different from the much more abundant "amber" zircons. The large ash-flow sheets of the central San Juan Mountains erupted over an interval of 3–4 millions years (Lipman et al., 1970), with the FCT approximately in the middle of this range. Contamination of FCT zircon with zircon from earlier eruptions or from earlier-formed zircon left in the subcaldera, upper crustal magma chamber is possible, and Pb and Sr isotopic data indicate significant contamination by upper crustal rocks (Lipman et al., 1978). Thus, we believe the TIMS result of 27.52 ± 0.09 Ma is the best U–Pb age obtainable from the presented data.

6. Summary and conclusions

The ages measured on minerals from the FCT using the K–Ar, Rb–Sr, and U–Pb decay schemes are in good agreement and give the following:

K–Ar and ^{40}Ar / ^{39}Ar total fusion:	27.57 ± 0.36 Ma
$^{40}Ar/^{39}Ar$ plateau and isochron:	27.57 ± 0.18 Ma
Rb–Sr biotite–feldspar isochron:	27.44 ± 0.16 Ma
U–Pb zircon discordia:	27.52 ± 0.09 Ma

The Rb–Sr FCT "biotite" analyses have been checked with standards and calibrated vs. NBS SRM 607 K-feldspar, and the "best" age of 27.44 ± 0.16 Ma seems to rest on a more solid reference basis than the zircon age. Although the biotite is also contaminated with inclusions, it appears that these inclusions do not yield significant amounts of extraneous radiogenic strontium, and the biotite data move along the isochron with increasing sample purification.

The K–Ar and $^{40}Ar/^{39}Ar$ data on various FCT minerals yield reasonably coherent ages. K–Ar biotite and hornblende ages are calculated directly from measured concentrations of K and Ar and do not depend on the age of a reference standard. The mean K–Ar age of 27.54 ± 0.27 Ma compares very well with the Rb–Sr age. Recent K–Ar measurements on FCT biotite in the Geological Survey of Japan laboratories have yielded ages of 27.5 ± 0.2 Ma for Ar measured by isotope dilution, and 27.4 ± 0.2 Ma for Ar measured by an "unspiked sensitivity method" (K. Uto, written communication, 1998).

The overall assessment of the ages measured using three independent decay schemes, K–Ar, Rb–Sr and U–Pb, suggests that the best age for FCT is 27.51 Ma and that all three dating methods yield comparable results.

Acknowledgements

H. B. is grateful to Charles Naeser for furnishing maps and information enabling him to collect the FCT at the original USGS sampling site. Many thanks are also due to W. Compston and I. Williams of the Research School of Earth Sciences, Australian National University for help in the preparation and carrying out of the FCT SHRIMP analyses. The TIMS analyses at the University of Alberta were facilitated by a major equipment grant (VG-354) and operating grants to H.B. from the National Sciences and Engineering Research Council of Canada.

Ar measurements were made by J.C. Von Essen and J.Y. Saburomaru and K measurements were made by B. Lai and M. Taylor. T.M. Debey and his staff irradiated the samples for $^{40}Ar/^{39}Ar$ dating.

The manuscript was improved by constructive comments from R.W. Kistler, J.L. Wooden, W.R. Van Schmus, and Ray Burgess.

References

Beckinsale, R.D., Gale, N.H., 1969. A reappraisal of the decay constants and branching ratio of ^{40}K. Earth Planet. Sci. Lett. 6, 289–294.

Cavell, P.A., 1986. The geochronology and petrogenesis of the Big Spruce Lake Alkaline Complex. Unpublished PhD thesis, University of Alberta, 448 pp.

Clark, G.J., Gulson, B.L., Cookson, J.A., 1979. Pb, U, Tl, Hf and Zr distributions in zircon determined by proton microprobe and fission track techniques. Geochim. Cosmochim. Acta 43, 905–918.

Compston, W., Williams, I.S., 1992. Ion probe ages from the British Ordovician and Silurian stratotypes. In: Webby, B.D., Laurie, J.R. (Eds.), Global Perspectives on Ordovician Geology. pp. 59–67, Balkema, Rotterdam.

Compston, W., Williams, I.S., Meyer, C., 1984. U–Pb geochronology of zircons from lunar breccia 73217 using a sensitive high mass-resolution ion microprobe. Proceedings of the 14th Lunar and Planetary Science Conference. . J. Geophys. Res. 89 (Suppl.), B525–B534.

Dalrymple, G.B., Duffield, W.A., 1988. High precision $^{40}Ar/^{39}Ar$ dating of Oligocene rhyolites from the Mogollon–Datil volcanic field using a continuous laser system. Geophys. Res. Lett. 15, 463–466.

Dalrymple, G.B., Lanphere, M.A., 1969. Potassium–Argon Dating. W.H. Freeman, San Francisco, 258 pp.

Davis, D.W., Gray, J., Cumming, G.L., Baadsgaard, H., 1977. Determination of the ^{87}Rb decay constant. Geochim. Cosmochim. Acta 41, 1745–1749.

Duke, M.J.M., 1993. The geochronology, geochemistry and isotope geology of the type-Nuk gneisses of the Akia terrane, southern West Greenland. Unpublished PhD thesis, University of Alberta, 286 pp.

Garner, E.L., Murphy, T.J., Gramlich, J.W., Paulsen, P.J., Barnes, I.L., 1976. Absolute isotopic abundance ratios and the atomic weight of a reference sample of potassium. J. Res. Natl. Bur. Stand., Sect. A 79 A, 713–725.

Hildreth, W., Lanphere, M.A., 1994. Potassium–argon geochronology of a basalt–andesite–dacite arc system: the Mount Adams volcanic field, cascade range of southern Washington. Geol. Soc. Am. Bull. 106, 1413–1429.

Jaffey, A.H., Flynn, K.F., Glendenin, L.F., Bentley, W.C., Essling, A.M., 1971. Precision measurements of half-lives and specific activities of ^{235}U and ^{238}U. Phys. Rev. C 4, 1889–1906.

Köppel, V., Grünenfelder, M., 1971. A study of inherited and newly-formed zircons from paragneisses and granitised sediments in the Strona–Ceneri-Zone (Southern Alps). Min. Petr. Mitteilungen 51, 385–410.

Krogh, T.E., 1973. A low contamination method for hydrothermal decomposition of zircon and extraction of U and Pb for isotopic age determinations. Geochim. Cosmochim. Acta 37, 485–494.

Krogh, T.E., 1982. Improved accuracy of U–Pb ages by the creation of more concordant systems using an air abrasion technique. Geochim. Cosmochim. Acta 46, 637–649.

Krogh, T.E., Davis, G.L., 1975. The production and preparation of ^{205}Pb for use as a tracer for isotope dilution analyses. Carnegie Institution of Washington Yearbook 1974, 416–417.

Lanphere, M.A., 2000. Comparison of conventional K–Ar and $^{40}Ar/^{39}Ar$ dating of young mafic volcanic rocks. Quat. Res. 53, 294–301.

Lanphere, M.A., and Dalrymple, G.B., 2000. First-Principles Calibration of ^{38}Ar Tracers: Implications for Ages of $^{40}Ar/^{39}Ar$ Fluence Monitors: US Geological Survey Professional Paper 1621, 10 pp.

Lipman, P.W., 1975. Evolution of the Platoro Caldera Complex and related volcanic rocks, Southeastern San Juan Mountains, Colorado. Geological Survey Professional Paper 852, 128 pp.

Lipman, P.W., Steven, T.A., Mehnert, H.H., 1970. Volcanic history of the San Juan Mountains, Colorado, as indicated by potassium–argon dating. Geol. Soc. Am. Bull. 81, 2329–2352.

Lipman, P.W., Doe, B.R., Hedge, C.E., Steven, T.A., 1978. Petrologic Evolution of the San Juan volcanic field, southwestern Colorado: Pb and Sr isotopic evidence. Geol. Soc. Am. Bull. 89, 59–82.

Ludwig, K.R., 1991. PBDAT: a computer program for processing Pb–U–Th isotope data, version 1.20. US Geological Survey Open-file Report 88-542.

Manton, W.I., 1988. Separation of Pb from young zircons by single-bead ion exchange. Chem. Geol. 73, 147–152, (Isotope Geoscience Section).

Mattinson, J.M., 1994. A study of complex discordance in zircons using step-wise dissolution techniques. Contrib. Mineral. Petrol. 116, 117–129.

McClelland, W.C., Mattinson, J.M., 1996. Resolving high precision U–Pb ages from Tertiary plutons with complex zircon systematics. Geochim. Cosmochim. Acta 60, 3955–3965.

McLaren, A.C., FitzGerald, J.D., Williams, I.S., 1993. The microstructure of zircon and its influence on the age determination from Pb/U isotopic ratios measured by ion microprobe. Geochim. Cosmochim. Acta 58, 993–1005.

Min, K., Mundil, R., Renne, P.R., Ludwig, K.R., 2000. A test for systematic errors in $^{40}Ar/^{39}Ar$ geochronology through comparison with U/Pb analysis of a 1.1-Ga rhyolite. Geochim. Cosmochim. Acta 64, 73–98.

Nasdala, L., Pidgeon, R.T., Wolf, D., 1995. Heterogeneous metamictization of zircon on a microscale. Geochim. Cosmochim. Acta 60, 1091–1097.

Oberli, F., Fischer, H., Meier, M., 1990. High-resolution $^{238}U/^{206}$Pb zircon dating of Tertiary bentonites and Fish Canyon Tuff: a test for age "concordance" by single crystal analysis. Seventh International Conference on Geochronology Cosmochronology and Isotope Geology. Geological Society of Australia Abstracts Number, vol. 27, 74.

Parrish, R.R., Krogh, T.E., 1987. Synthesis and purification of ^{205}Pb for U–Pb geochronology. Chem. Geol. 66, 103–110, (Isotope Geoscience Section).

Parrish, R.R., Roddick, J.C., Loveridge, W.D., Sullivan, R.W., 1987. Uranium-lead analytical techniques at the geochronology laboratory, Geological Survey of Canada. In: Radiogenic Age and Isotopic studies: Geological Survey of Canada Report 1, Paper 87-2, 3–7.

Paterson, B.A., Stephens, W.E., Rogers, G., Williams, I.S., Hinton, R.W., Herd, D.A., 1992. The nature of zircon inheritance in two granite plutons. Trans. R. Soc. Edinburgh: Earth Sci. 83, 459–471.

Pidgeon, R.T., 1992. Recrystallisation of oscillatory zoned zircon: some geochronological and petrological implications. Contrib. Mineral. Petrol. 110, 463–472.

Renne, P.R., Swisher, C.C., Deino, A.L., Karner, D.B., Owens, T.L., DePaolo, D.J., 1998. Intercalibration of standards, absolute ages, and incertainties in $^{40}Ar/^{39}Ar$ dating. Chem. Geol. 145, 117–152.

Roddick, J.C. and van Breemen, O., 1994. U–Pb zircon dating: a comparison of ion microprobe and single grain conventional analyses; in: Radiogenic Age and Isotope Studies: Report 8; Geological Survey of Canada, Current Research 1994-F, 1–9.

Sergeev, S.A., Meier, M., Steiger, R.H., 1995. Improving the resolution of single-grain U/Pb dating by use of zircon extracted from feldspar: application to the Variscan magmatic cycle in the central Alps. Earth Planet. Sci. Lett. 134, 37–51.

Shields, W.R., 1960. Comparison of Belgian Congo and Synthetic "Normal" Samples. Table 6 in Appendix A. Report no. 8, U.S. National Bureau of Standards Meeting of the Advisory Committee for Standard materials and Methods of Management, May 17 and 18 (1960) 37 pp. (unpublished).

Sommerauer, J., 1974. Trace element distribution patterns and the mineralogical stability of zircon—an application for combined electron microprobe techniques. Electron Microsc. Soc. South Afr., Proc. 4, 71–72.

Stern, R.A., 1997. The GSC Sensitive High Resolution Ion Microprobe (SHRIMP): analytical techniques of zircon U–Th–Pb age determinations and performance evaluation. In: Radiogenic Age and Isotope Studies: Report 10; Geological Survey of Canada, Current Research 1997-F, 1–31.

Steiger, R.H., Bickel, R.A., Meier, M., 1993. Conventional U–Pb dating of single fragments of zircon for petrogenetic studies of Phanerozoic granitoids. Earth Planet. Sci. Lett. 115, 197–209.

Taylor, J.R., 1982. An Introduction To Error Analysis. University Science Books, Mill Valley, 270 pp.

Tera, F., Wasserburg, G.J., 1972. U–Th–Pb systematics in three Apollo 14 basalts and the problem of initial Pb in lunar rocks. Earth Planet. Sci. Lett. 14, 281–304.

Watson, E.B., Cherniak, D.J., Hanchar, J.M., Harrison, T.M., Wark, D.A., 1997. The incorporation of Pb into zircon. Chem. Geol. 141, 19–31.

Whitney, J.A., Stormer, J.C., 1985. Mineralogy, petrology, and magmatic conditions from the Fish Canyon Tuff, Central San Juan Volcanic Field, Colorado. J. Petrol. 26, 726–762.

Williams, I.S., 1992. Some observations on the use of zircon U–Pb geochronology in the study of granitic rocks. Trans. R. Soc. Edinburgh: Earth Sci. 83, 447–458.

Williams, I.S., Claesson, S., 1987. Isotopic evidence for the provenance and Caledonian Metamorphism of high grade paragneisses from the Seve Nappes, Scandinavian Caledonides: ion microprobe zircon U–Th–Pb. Contrib. Mineral. Petrol. 97, 205–221.

York, D., 1969. Least squares fitting of a straight line with correlated errors. Earth Planet. Sci. Lett. 5, 320–324.